

Research Article

Open Access



Mechanically flexible and flame-retardant cellulose nanofibril-based films integrated with MXene and chitosan

Shi-Neng Li^{1,*,#}, Zi-Fan Zeng^{1,#}, Xiao-Feng He¹, Zhi-Chao Xu¹, Yu-Hang Luo¹, Qing-Yue Ni¹, Li Peng^{2,*}, Li-Xiu Gong³, Yang Li⁴, Baiyu Jiang^{1,*}

¹College of Chemistry and Materials Engineering, Zhejiang A & F University, Hangzhou 311300, Zhejiang, China.

²School of Micro-Nano Electronics, Zhejiang University, Hangzhou 311200, Zhejiang, China.

³Key Laboratory of Organosilicon Chemistry and Material Technology of Ministry of Education, College of Material, Chemistry and Chemical Engineering, Hangzhou Normal University, Hangzhou 311121, Zhejiang, China.

⁴Department of Nano-physics, Gachon University, Seongnam-si, Gyeonggi-do 13120, Korea.

#Authors contributed equally.

***Correspondence to:** Dr. Shi-Neng Li, College of Chemistry and Materials Engineering, Zhejiang A & F University, 666 Wusu Street, Lin'an District, Hangzhou 311300, Zhejiang, China. E-mail: lisen@zafu.edu.cn; Prof. Li Peng, School of Micro-Nano Electronics, Zhejiang University, 733 Jianshesan Road, Xiaoshan District, Hangzhou 311200, Zhejiang, China. E-mail: l-peng@zju.edu.cn; Dr. Baiyu Jiang, College of Chemistry and Materials Engineering, Zhejiang A & F University, 666 Wusu Street, Lin'an District, Hangzhou 311300, Zhejiang, China. E-mail: jiangby@zafu.edu.cn

How to cite this article: Li SN, Zeng ZF, He XF, Xu ZC, Luo YH, Ni QY, Peng L, Gong LX, Li Y, Jiang B. Mechanically flexible and flame-retardant cellulose nanofibril-based films integrated with MXene and chitosan. *Soft Sci* 2022;2:21. <https://dx.doi.org/10.20517/ss.2022.20>

Received: 16 Sep 2022 **First Decision:** 14 Oct 2022 **Revised:** 16 Nov 2022 **Accepted:** 23 Nov 2022 **Published:** 6 Dec 2022

Academic Editors: Zhifeng Ren, Chuan Fei Guo **Copy Editor:** Fangling Lan **Production Editor:** Fangling Lan

Abstract

Remarkable flame-retardant and integrated mechanical properties are essential requirements for the potential applications of bio-based films in industrial areas. Unfortunately, the design and fabrication of such film materials that possess a good trade-off between mechanical properties and flame-retardant performance remain significant challenges. Here, phosphorylated cellulose nanofibril-based films (PCNFs) integrated with chitosan (CS) and MXene (PCNF/CS-M) are fabricated via a facile water evaporation-induced self-assembly method. An evident reinforcement of the mechanical performance can be achieved by constructing additional interactions (i.e., hydrogen bonding and nanoreinforcement) among the hybrid network, which endows the optimized films with highly improved and balanced mechanical performance (i.e., tensile strength of 172.1 MPa, tensile strain of 8.0%, Young's modulus of 4.4 GPa and toughness of 8.5 MJ/m³). Furthermore, the resultant films also exhibit outstanding flame resistance, as clearly illustrated by their structural integrity after cyclic testing using a butane



© The Author(s) 2022. **Open Access** This article is licensed under a Creative Commons Attribution 4.0 International License (<https://creativecommons.org/licenses/by/4.0/>), which permits unrestricted use, sharing, adaptation, distribution and reproduction in any medium or format, for any purpose, even commercially, as long as you give appropriate credit to the original author(s) and the source, provide a link to the Creative Commons license, and indicate if changes were made.



lamp flame at 700-800 °C. The synergistic reinforcing and flame-retardant mechanisms of the films are clarified based on structural evolution and performance variation. The strategy developed herein provides an innovative concept for designing and developing advanced bio-based film materials for fireproof coatings.

Keywords: Phosphorylated cellulose nanofibrils, film materials, chitosan, Mxene, mechanical properties, flame resistance

INTRODUCTION

Polymer materials based on natural biopolymers (e.g., starch, alginate, and so on)^[1-4] that integrate mechanical flexibility, biodegradability and inexpensiveness are of great importance for achieving the goals of carbon neutrality and sustainable development. Cellulose nanofibrils (CNFs), as bio-based nanomaterials with a filamentous morphology^[5] and tunable surface charge characteristics^[6], have attracted tremendous research interest due to their abundant reserves and excellent overall performance^[7,8]. Compared to conventional biopolymers, the unique nanoscale and hydrophilic features of CNFs empower them with a high aspect ratio, good water dispersibility and favorable processibility^[9-11]. Therefore, they are promising candidates for achieving film materials with good integrated performance, including high stretchability and transparency. Unfortunately, due to their inherently inflammable nature, CNF-based film structures are easily disaggregated when directly exposed to heat corrosion or flame attack, resulting in major obstacles to their development and applications from bench to market. Thus, it remains a significant challenge to develop novel CNF-based films with excellent flame-retardant performance.

To tackle the above issue, various strategies have been continuously explored in recent years, such as chemical treatment with phosphorus-containing reagents^[12] and introducing flame-retardant compounds^[13,14] and nanomaterials^[15] into the matrix. However, when using a single strategy, achieving a good trade-off between mechanical properties and flame-retardant performance is challenging. As an exciting family of layered nanomaterials, MXene (two-dimensional transition-metal carbides and/or nitrides) sheets have triggered extensive research in a vast array of applications due to their high aspect ratio morphology and excellent mechanical performance^[16]. Interestingly, MXenes also exhibit outstanding flame resistance and good water dispersibility because of their inorganic backbone and rich surface hydrophilic moieties^[17]. Considering the typical method, i.e., the water evaporation-induced self-assembly process, for fabricating CNF-based films^[18], as nanofillers, integrating CNFs with MXenes (water system) is a reasonable approach to obtain flame-retardant composite materials. Li *et al.* developed an improved flame-resistant composite aerogel composed of lignocellulose nanofibrils, MXene and gelatin^[19]. Notably, the mechanical performance of the aerogel was not desirable, e.g., a weakened recovery ability, which is closely related to the interactions among components. Therefore, regulating and controlling the corresponding interactions between CNFs and MXenes is crucial to achieving CNF-based composite films with balanced mechanics and exceptional flame resistance, but this has not yet been reported in the literature.

Here, we report mechanical flexible CNF-based films with flame retardancy reinforced by MXene and chitosan based on a water evaporation-induced self-assembly method. The obtained films show highly improved and balanced mechanical properties, i.e., high tensile strength and toughness. This is mainly attributed to the formation of a homogeneous and highly aligned structure after modulating multiple interactions among the components, as verified by the structural results (i.e., evolution morphology and chemical structure). Furthermore, the effect of chitosan and MXene contents on the mechanical behavior is systematically investigated based on the results of mechanical tests. In addition, compared with the poor structural stability of a pure PCNF film, the PCNF/CS-M film possesses outstanding flame resistance during

cyclic testing with a butane lamp flame. Finally, based on the structural evolution, flame-retardant measurements and corresponding analysis, the flame-retardant mechanism is clarified to understand the structure-property relationship of the films.

EXPERIMENTAL

Materials

A Ti_3AlC_2 precursor was purchased from Jilin Technology Co., Ltd. Pulp sheets with a cellulose content of 95.9 wt.% were purchased from Hangzhou Bamfox Bamboo Products Co., Ltd. and sifted through a metal-based sieve (100 mesh) before further use. CS (degree of deacetylation $\geq 95\%$, viscosity of 100-200 mPa/s), diammonium hydrogen phosphate ($(\text{NH}_4)_2\text{HPO}_4$), lithium fluoride salt (LiF, ≥ 98 wt.%), hydrochloric acid (HCl, 35 wt.%), urea and other chemicals were purchased from Aladdin Co., Ltd. (China). All chemicals were used without further purification.

Fabrication of phosphorylated cellulose nanofibril/chitosan-MXene films

The phosphorylated CNF/CS-MXene films were fabricated via solvent casting (see the details in [Supplementary Table 1](#)). Phosphorylated cellulose nanofibrils and $\text{Ti}_3\text{C}_2\text{T}_x$ MXene nanosheets were prepared according to our previous works^[16,20] and the structural and morphological characterization results are shown in [Supplementary Figures 1-3](#). The fabrication process of the composite films is described as follows. In brief, a certain volume of MXene aqueous solution was slowly added to a PCNF suspension and a uniform mixture was obtained under mechanical stirring. After that, a certain amount of CS was introduced into the above solution and further stirred until a homogeneous suspension was formed. The suspension was then stored in a vacuum oven with a fixed temperature of 45 °C. Finally, a dark film could be obtained after 72 h of the evaporation-induced self-assembly process. The resultant films were labeled as PCNF/CSx-My, with CS for chitosan and M for MXene, respectively. Notably, x represents the content of CS and y is for the solid content of MXene in the suspension. As controlled samples, the PCNF and PCNF films with CS or MXene were also prepared through the same fabrication process.

Characterization

To understand the chemical structure, the PCNF films were characterized at the scanning range of 4000 to 400 cm^{-1} using Fourier transform infrared spectroscopy (FTIR, Nicolet6700, Thermo, USA). The surface compositions of the PCNF films were analyzed by X-ray photoelectron spectroscopy (XPS) (K-Alpha, Thermo Fisher Scientific, USA) under an ultrahigh vacuum. The morphology of the CNFs was characterized by transmission electron microscopy (JEM-1200EX, JEOL, Japan). The thermal stability was explored by thermogravimetric analysis (TG209F1, Netzsch, Germany) from 35 to 800 °C at a heating rate of 10 °C/min in an air atmosphere. The morphology of the microstructures of the cellulose films was investigated by scanning electron microscopy (SEM, SU8010, Hitachi, Japan). Thermogravimetric analysis-infrared spectroscopy was carried out using a PerkinElmer TGA 4000 thermogravimetric analyzer connected to a PerkinElmer Spectrum Two FTIR spectrometer. The gaseous degradation volatiles were detected during the process of thermal degradation.

Mechanical measurements

Tensile measurements were conducted on specimens (length of 30 mm and width of 5 mm) using a mechanical testing machine (SANS CMT6104, MTS, USA) equipped with a 100 N load cell at a test speed of 1 $\text{mm} \cdot \text{min}^{-1}$. The tensile strength was determined as $\sigma = F/A_0$, where F and A_0 represent load force and original cross-sectional area, respectively. The tensile strain was defined as $\varepsilon = \Delta l/l_0 \times 100\%$, where Δl is the change in length relative to the initial length (l_0). The Young's modulus was calculated by fitting the initial linear regime of the stress-strain curve. The toughness was estimated by the area under the tensile stress-strain curve.

Microscale combustion calorimetry

The microscale combustion calorimeter (FAA-PCFC, Fire Testing Technology, UK) experiments were conducted with MCC measurements. The tested specimen weighing ~5 mg was heated to 650 °C at a heating rate of 1 °C/min with a nitrogen flow stream of 80 mL/min. The thermal degradation products were mixed with a 20 mL/min stream of oxygen before entering a 900 °C combustion furnace.

RESULTS AND DISCUSSION

The fabrication processes of the composite films are revealed in [Figure 1](#), including the nanofibration of pulp sheets, Ti_3AlC_2 delamination and the water evaporation-induced self-assembly process. In brief, CS and MXene were introduced into a PCNF water solution, which could be obtained by combining the mechanical grinding process and chemical pre-treatment to form a homogeneous solution under continuous stirring. A paper-like film was then obtained successfully with the aid of the water evaporation process. Owing to the presence of abundant hydrophilic groups in such a system, including amino- (CS), hydroxyl-, fluorine- (MXene) and phosphorus (PCNF)-containing groups, strong hydrogen bonding can be formed between PCNFs, CS molecules and MXene nanosheets, as shown in [Figure 1](#). Consequently, the resultant film displays both mechanical strength and flexibility that can sustain complex deformation, e.g., shaping to a paper plane, quadruple folding and twisting around a glass bar (diameter of ~4 mm) [[Supplementary Figure 4](#)]. Notably, there is no mechanical failure, including cracks or damage, during the operational process. Additionally, another inspiring feature is the highly improved flame retardance. Specifically, the as-prepared film cannot be ignited when brought into contact with a butane lamp flame (temperature of 700–800 °C). Furthermore, it retains a good macromorphology, even after repeatedly undergoing flame attack, as discussed in the following section. Considering the above advantages, these composite films may hold application potential as nonflammable film materials or efficient fireproof nanocoatings for combustible materials.

High mechanical strength and ductility are two crucial parameters for the practical application of film materials^[21–23]. Thus, the material components (i.e., CS and MXene contents) in the system were systematically investigated to achieve desirable performance through evaluation with a series of mechanical standard tests. As shown in [Figure 2A](#), the presence of CS or MXene improves the mechanical parameters, except for a slight decrease in strain. Notably, the combination of CS and MXene endows the PCNF/CS₅-M_{2.5} film with highly enhanced mechanical properties, which vastly exceed those of PCNF films integrated with CS or MXene alone [[Figure 2B](#) and [Supplementary Table 2](#)]. This phenomenon can be attributed to the synergistic effect of physical interactions (hydrogen bonding) and nanoparticle reinforcement^[24–26]. After regulating and optimizing the CS concentration and MXene content [[Figure 2C](#) and [D](#) and [Supplementary Tables 3 and 4](#)], the corresponding tensile strength, tensile strain, Young's modulus and toughness of the PCNF/CS-M film were further increased up to 172.1 MPa, 8.0%, 4.4 GPa and 8.5 MJ/m³, respectively. Based on these results, a tensile strength-toughness chart for other reported flame-retardant films^[27–31] was also derived [[Figure 2E](#)], as summarized in [Supplementary Table 5](#). Comparatively, it is apparent that the PCNF/CS-M film achieves both high strength and toughness and can also maintain impressive strain. This good trade-off between mechanical parameters expands the application range of flame-retardant film materials in future applications.

The corresponding structural evolution containing the chemical structure and morphology was investigated to gain insights into the strengthening mechanism. As shown in the FTIR spectra [[Figure 3A](#)], an apparent shift in the characteristic peak (3338 cm⁻¹) assigned to -OH indicates the occurrence of hydrogen bonding between the CS molecule and PCNFs^[32]. This peak is further shifted to a lower wavenumber (3280 cm⁻¹) after introducing the MXene, demonstrating that the functional groups (hydroxyl- and fluorine-containing

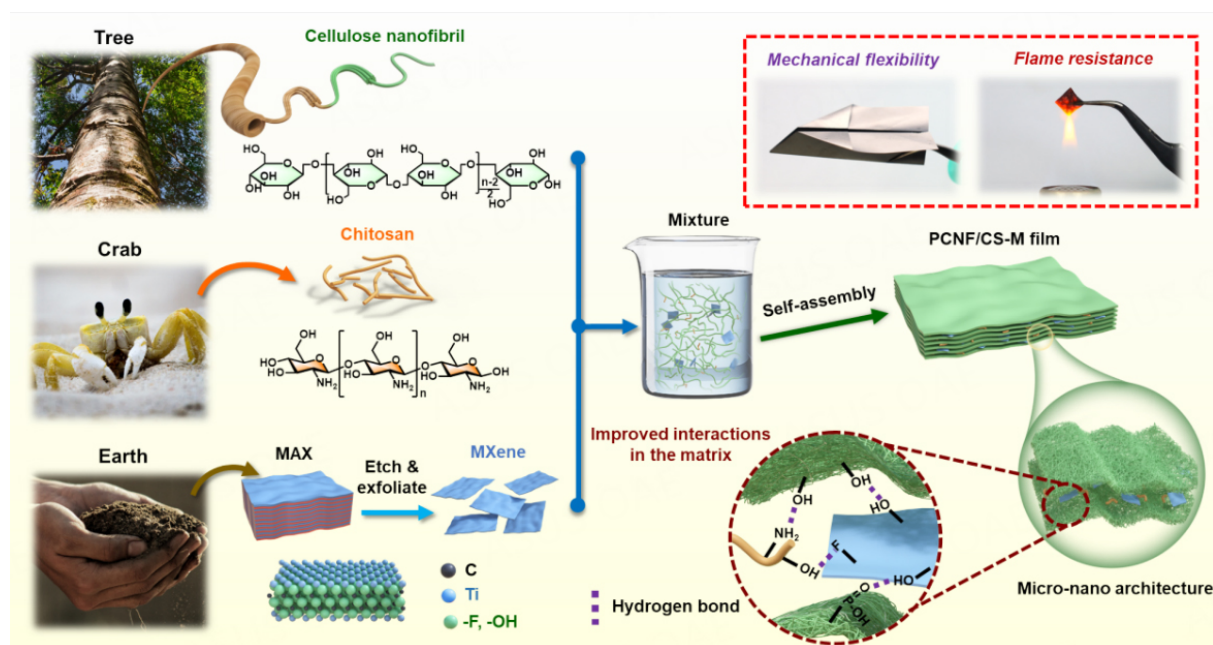


Figure 1. Schematic illustration of PCNF/CS-M film fabrication process based on water evaporation-induced self-assembly method.

groups) of the two-dimensional nanosheets should be involved in the formation of additional hydrogen bonds^[33]. In addition, the increased C-O (286.5 and 532.9 eV) in the C1s and O1s XPS spectra [Figure 3B and Supplementary Figure 5] further confirms the formation of strong hydrogen bonding in the PCNF/CS-M. More importantly, the evolution of interaction in the matrix can also be reflected by the internal microstructure. Compared to the lamellated structure with the relatively smooth fracture architecture of the virgin one [Figure 3C(i)], PCNF/CS₁₅-M_{5,0} exhibits a homogeneous and highly aligned structure after mechanical fracture. Interestingly, many river-like grooves on the cross section at a higher amplification [Figure 3C(ii)] reveal a typical sign of ductile fracture, which agrees well with the improved mechanical performance. Furthermore, as observed by the SEM images, a crack with related smooth cross-sectional structure appears on the surface of the PCNF film and straightly propagates through the matrix without an obvious deflection [Supplementary Figure 6]. In stark contrast, a crack with several apparent deflections (dark red arrows in Figure 3D) can be observed on the surface of the PCNF/CS-M film, indicating the evident deflection effect induced by the MXene nanosheets. With higher magnification, a terrace-like morphology with a visible saw-like structure) can be found on the edge of the cross section of the film, which is mainly induced by the presence of MXene nanosheets.

Based on the above results and analysis, a possible crack extension model is proposed, as displayed in Figure 3E. When subjected to applied stress, the PCNFs begin to slide over each other easily due to the absence of strong interactions and a crack appears and propagates with applied time. Furthermore, the flexible feature of PCNFs cannot restrain the growth and propagation of the crack, finally leading to a brittle rupture. Comparatively, a plethora of hydrogen bonds attributed to CS chains results in a strong association between the PCNFs and MXene nanosheets, resulting in significantly more energy being absorbed during the crack propagation. Once in contact with a MXene nanosheet, crack growth would be restricted and the occurrence of a deflection phenomenon induced due to its high mechanical stiffness, resulting in significantly more energy being absorbed during the crack propagation. Specifically, the propagating crack would be deflected by MXene nanosheets and propagate along the adjacent nanosheets. Before the mechanical failure, this crack deflection-propagation cycling always happens persistently, resulting in a

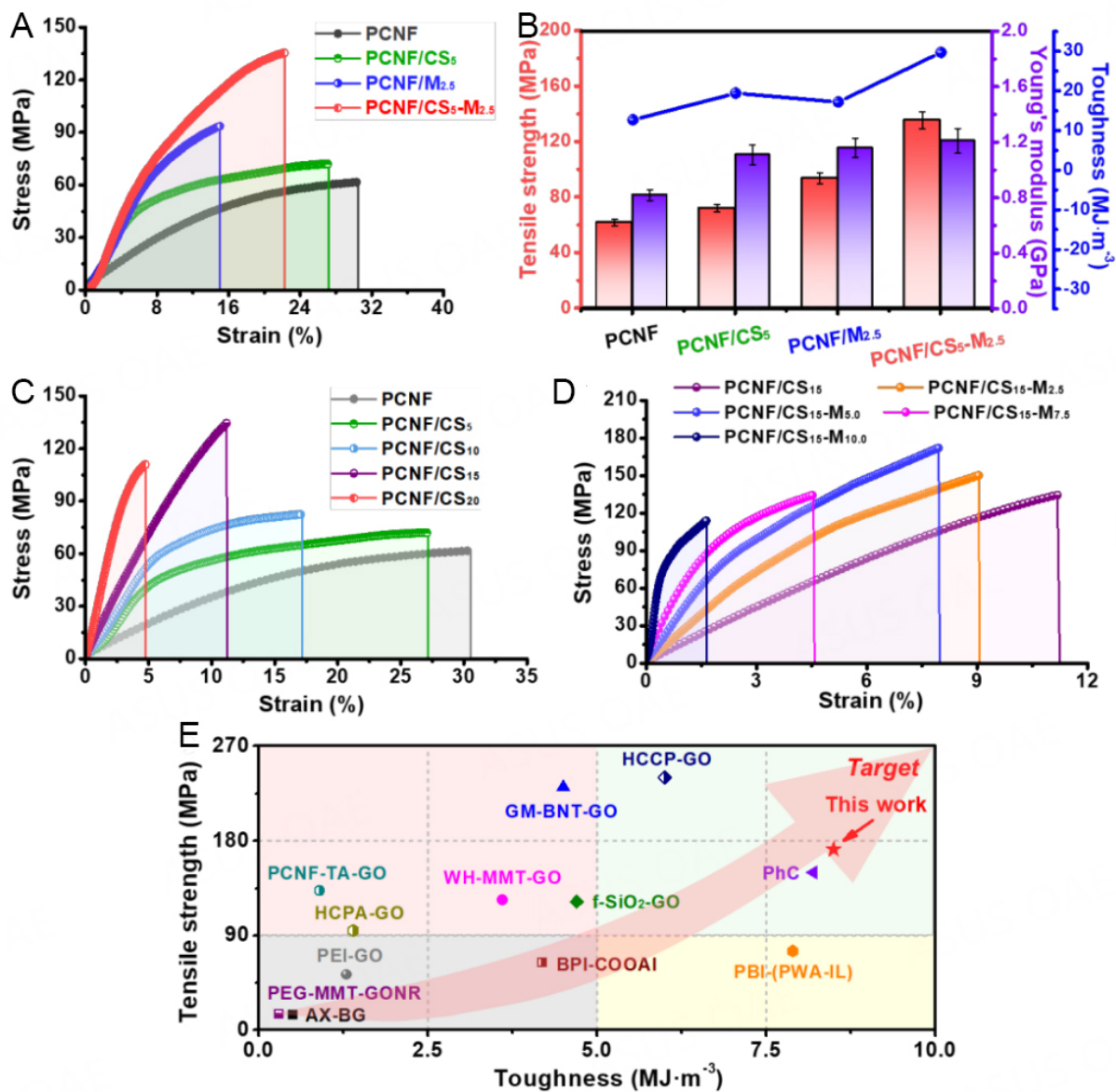


Figure 2. Mechanical optimization of PCNF/CS-M films. (A) Stress-strain curves and (B) corresponding parameters of obtained films with different compositions. (C) Stress-strain curves of obtained films with different CS concentrations. (D) Stress-strain curves of obtained films with different MXene contents. (E) Ashby-style plot comparing tensile strength and toughness of PCNF/CS-M film with those of other flame-retardant films reported in the literature.

unique microstructure, as observed in the SEM results [Figure 3D(i and ii)]. Therefore, a feature of integrated high strength and toughness can be achieved for the PCNF/CS-M film.

Considering the presence of phosphorus-containing groups and MXene nanosheets, the flame retardancy of the composite films was studied under a butane lamp flame (700–800 °C) with cyclic testing. Obviously, the PCNF film exhibits a rapid thermal decomposition when in contact with the flame with high temperature and self-extinguishing behavior once deviating from the flame [Figure 4A], which benefits from the formation of protective layers composed of P_xO_y and carbon^[20]. However, this film can still be completely burned out by the early stage of the second cycle, thereby revealing its relatively poor high-temperature

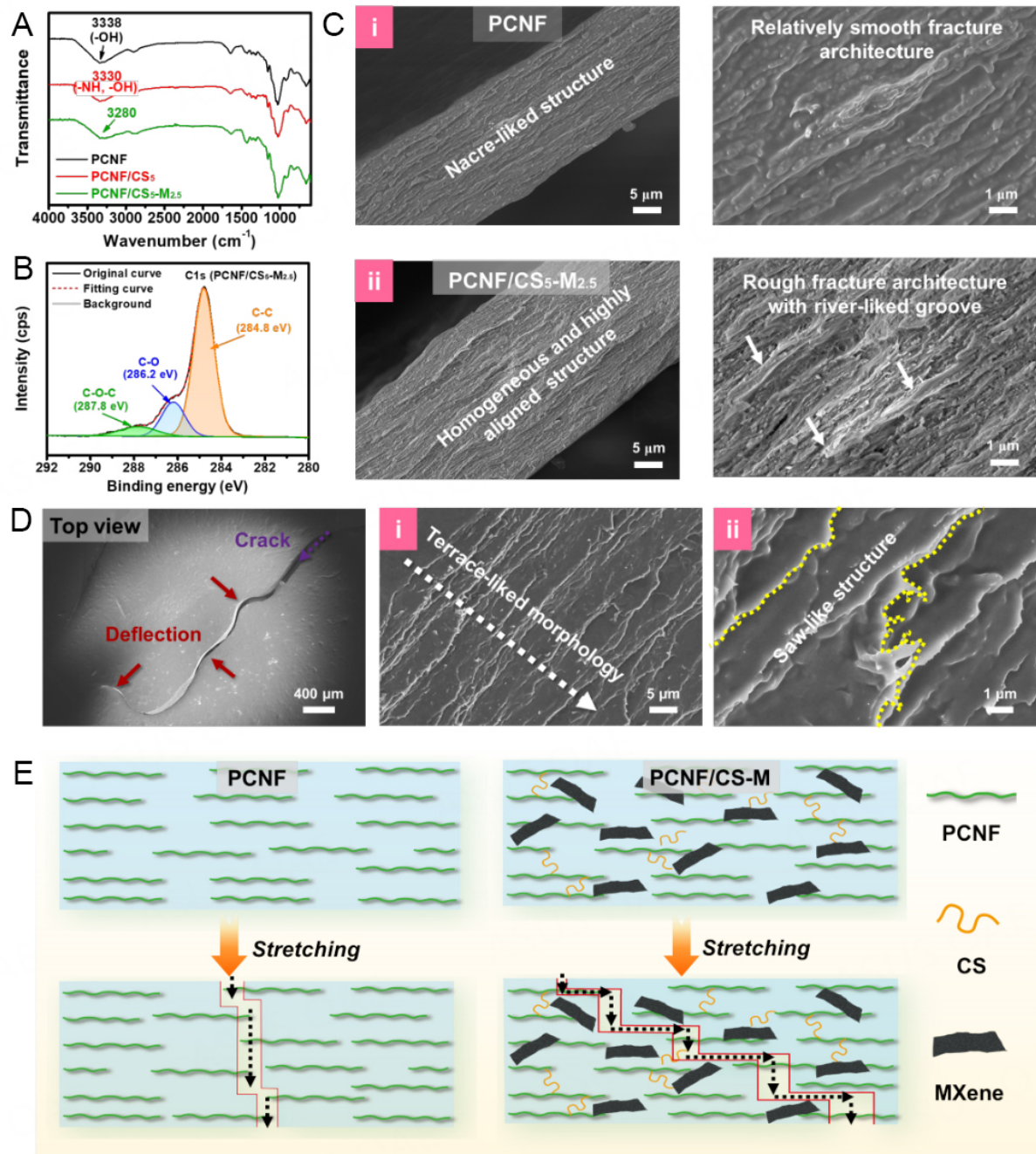


Figure 3. Morphological characterization and evolution of chemical structure of PCNF/CS-M films. (A) FTIR spectra of PCNF, PCNF/CS₅ and PCNF/CS₅-M_{2.5} films. (B) C1s XPS spectra of PCNF/CS₅-M_{2.5} films. (C) SEM images of cross-sectional morphology: (i) PCNF; (ii) PCNF/CS₅-M_{2.5} films. For PCNF/CS₅-M_{2.5}, the rough fracture architecture with river-like grooves indicates improved interactions in the matrix. (D) SEM images of PCNF/CS-M film after simple stretching. (E) Proposed synergistic reinforcement mechanism of PCNF/CS-M films.

resistance during cyclic flame testing. In marked contrast, the PCNF/CS-M film can retain shape and structural integrity even after four consecutive cycles [Figure 4B], implying the favorable role of CS and MXene in enhancing the flame-resistant performance. The corresponding FTIR results confirm this phenomenon [Supplementary Figure 7], as clearly certified by the difference (disappearance for the PCNF

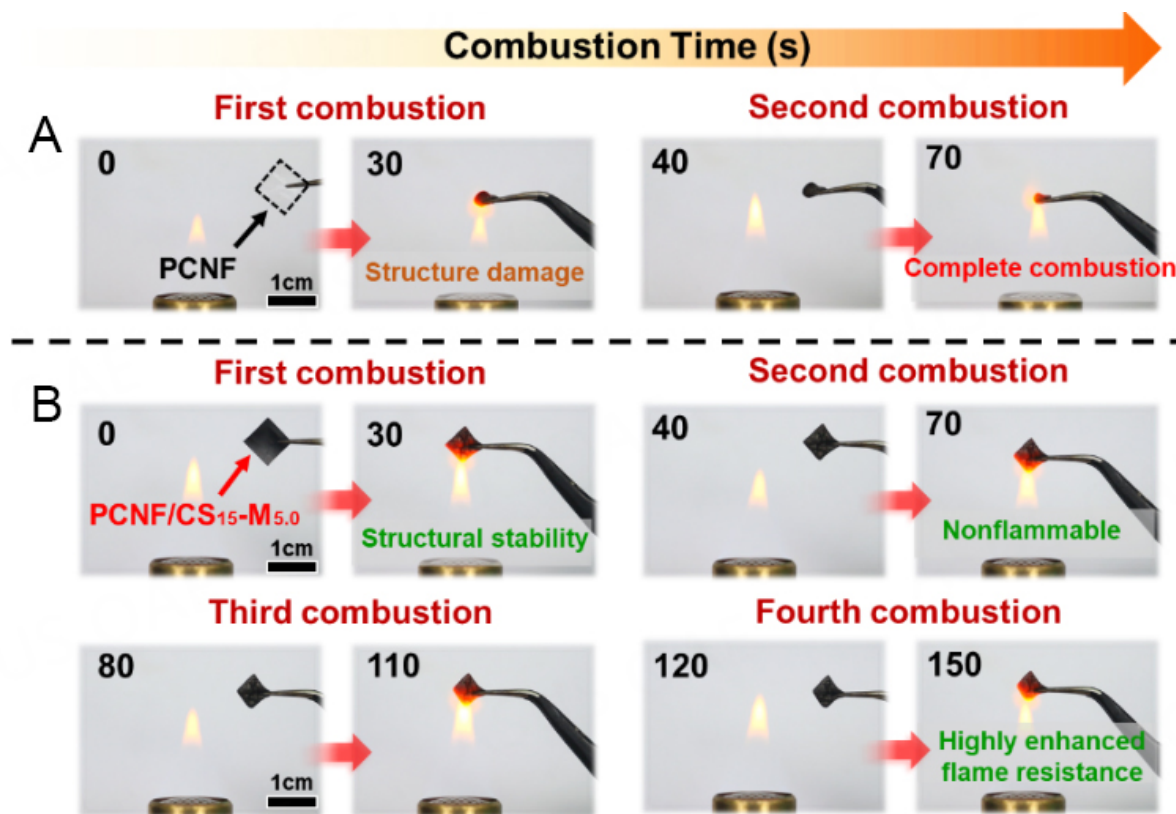


Figure 4. Flame-retardant performance. Cyclic combustion process of (A) PCNF and (B) PCNF/CS₁₅-M_{5.0} film, demonstrating highly improved flame resistance by incorporation of CS and MXene.

film and a minor change for the PCNF/CS-M film) in the characteristic peaks of the oxygen-containing groups. Owing to its outstanding flame-retardant property, PCNF/CS-M (PCM) hybrid networks can be used as flame-retardant nanocoatings for combustible materials, e.g., polyurethane (PU) foam via a facile tip-coating method. As displayed in [Supplementary Figure 8](#), flame combustion tests were conducted to evaluate the flame-retardant performance of a PU foam-coated PCM nanocoating (PCM-PU) (35 wt.% PCM, with respect to the weight of pure PU foam). Clearly, within a short time of 10 s, pure PU foam exhibits a typical combustion process of the polymer composite [[Supplementary Figure 8\(i\)](#)], including rapid ignition, violent burning with a vast amount of melt drippings and disappearing completely. Remarkably, no flame spreading and melt dripping could be observed in the PCM-PU foam [[Supplementary Figure 8\(ii\)](#)]. Even when increasing the time up to 90 s, the sample can still retain its integrated shape and self-extinguishing performance within 1 s, thereby demonstrating the highly enhanced flame retardancy of the PU foam. Therefore, such PCNF/CS-M hybrid networks exhibit application potential as effective fireproof nanocoatings for improving the flame resistance of flammable materials.

To further understand the inherent mechanism of flame retardancy in these films, the investigation of structural evolution containing morphology and chemical structure is an effective means^[34,35]. As shown in [Figure 5A](#), compared to the unburned area of the PCNF/CS₁₅-M_{5.0} film, the thickness of the burned area shows a distinct increase (172%, [Figure 5B\(i\)](#) and [Supplementary Figure 9](#)), which is a typical indicator of self/intumescent behavior due to the generation and release of nonflammable gases (H₂O, CO, and CO₂) being exposed to the flame environment^[26,36]. Interestingly, a compact and integrated cross section [[Figure 5B\(ii\)](#)] embedded with smaller nanoparticles [[Figure 5B\(iii\)](#)] can be obtained after incorporating

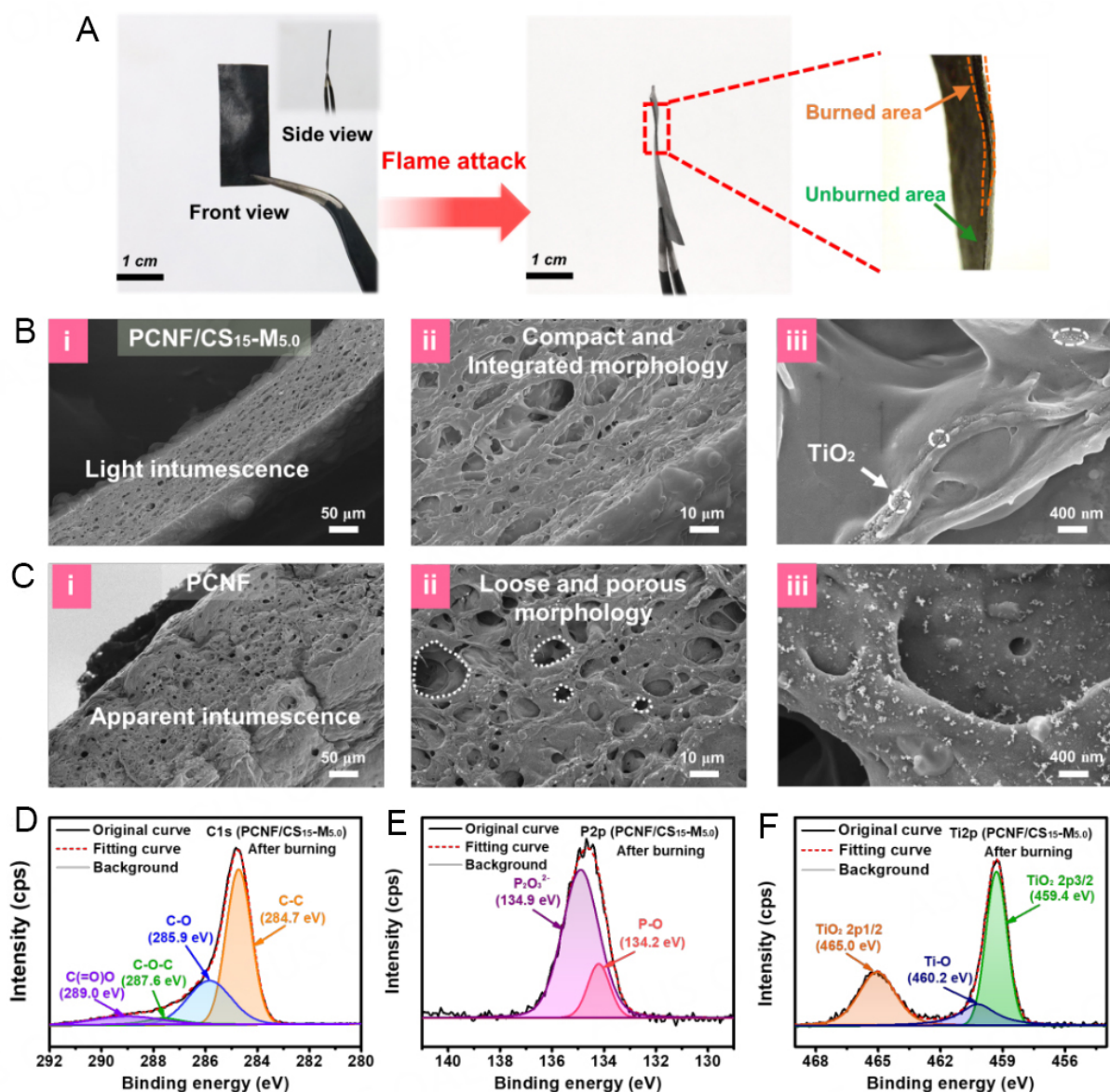


Figure 5. Structural evaluation of composite films after burning. (A) Digital photographs of PCNF/CS₁₅-M_{5.0} film before/after being exposed to butane flame. Cross-sectional SEM images of (B) PCNF/CS₁₅-M_{5.0} and (C) PCNF films after flame attack. (D) C1s, (E) P2p and (F) Ti2p XPS spectra of PCNF/CS₁₅-M_{5.0} film after burning.

MXene nanosheets and CS molecules, in accordance with the excellent flame resistance discussed above [Figure 4B]. A similar but different phenomenon (a larger change of 676% in thickness, Supplementary Figure 9) can also be observed, as clearly reflected by the cross-sectional SEM image of the PCNF film [Figure 5C(i) and Supplementary Figure 10]. From careful observation, many nanoparticles that appear on the surface with a loose and porous morphology [Figure 5C(ii and iii)] should be P_xO_y derived from the thermal decomposition and dehydration of phosphorus-containing groups^[20], as discussed below.

From further analysis of the XPS results, it is revealed that all the typical peaks of the PCNF/CS₁₅-M_{5.0} film containing C1s, O1s, N1s, P2p, and Ti2p are retained after the burning treatment [Supplementary Figure 11A]. Furthermore, an apparent change in the intensities and shapes of the P2p and

Ti2p peaks can be observed, signifying the generation of new compounds during burning [Supplementary Figure 11B-G]. The decreased intensity of oxygen-containing groups [Figure 5D and Supplementary Figure 11H and I] provides insight into the occurrence of thermal degradation. Additionally, the ratio of P-O to $P_2O_3^{2-}$ increases after burning [Figure 5E and Supplementary Figure 11J], implying the formation of P_xO_y and a char layer through thermal transformation. Notably, the higher residual char of the PCNF/CS-M film [Supplementary Figure 12 and Supplementary Table 6] elucidates its improved thermal stability and enhanced char-forming capability. The disappearance of the Ti-C and Ti-O ($2p\ 3/2$) peaks and largely increased intensity of the characteristic peaks at 459.4 and 460.0 eV [Figure 5F and Supplementary Figure 11K] reveal the successful generation of nano-TiO₂ during the ignition process. These findings strongly support the results of the SEM images. In conclusion, the outstanding flame resistance of the PCNF/CS-M film lies in the combination of P_xO_y , char and TiO₂ nanoparticles. This can be explained by the thermal transformation of the phosphorus-containing group and the oxidation behavior of the MXene nanosheets under continuous flame attack.

To quantitatively analyze the flame-retardant performance of the PCNF/CS-M films, two facile and valuable technologies, namely, microscale combustion calorimetry (MCC) and thermogravimetric analysis-infrared spectroscopy, were utilized. The detailed data are summarized in Supplementary Table 7. For the curves plotted by the MCC data, the presence of MXene and CS empowers PCNF/CS-M_{5.0} with a low peak heat release rate (70.8 W/g), total heat release (5.3 kJ/g) and heat release capacity (70.0 J/g/K) [Figure 6A and B and Supplementary Table 7], corresponding to decreases of 25.6%, 20.9% and 24.7% compared to pure PCNF films, respectively. This was further proven by the increased residual carbon [Supplementary Figure 12 and Supplementary Table 6]. These results show that the PCNF/CS-M films possess the advantages of lower combustion enthalpy and high char-forming capability due to the eminent barrier effect of the hybrid layer composed of P_xO_y , char and TiO₂ nanoparticles. It is noteworthy that the inherent mechanism of flame-retardant materials can also be evaluated from the evolution of the corresponding pyrolytic composition. As shown in Figure 6C, gases (nonflammable H₂O, CO and CO₂ and flammable hydrocarbons) and pyrolysis compounds are generated during thermal degradation. Importantly, the total and characteristic absorptions assigned to the hydrocarbons and carbonyl compounds of the PCNF/CS-M film are all lower than those of the virgin ones [Supplementary Figure 13], revealing evidence of the suppressed formation or release of flammable gases^[37]. Furthermore, the appearance of the characteristic peak corresponding P=O at 1273 cm⁻¹ indicates the free radical capturing effect produced by phosphorus-containing groups in the gas phase^[38].

According to the above analysis and discussion, a possible flame-retardant mechanism of the PCNF/CS-M film is proposed and illustrated in Figure 6D. Generally, owing to the thermal decomposition of oxygen- and nitrogen-containing groups, abundant gases can be generated and released from the polymer matrix, thus leading to a porous architecture, i.e., intumescent behavior from a macroscopic perspective. In terms of condensed-phase flame retardancy, phosphorus-containing groups in PCNF can serve as char promoters and free radical capturers^[39] during combustion, thereby achieving a highly compact carbon layer by facilitating the carbonization process of cellulose chains and interrupting the chain reaction^[40,41]. Additionally, nano P_xO_y phases that effectively protect the polymer network from fire and heat damage are also obtained simultaneously [Figure 5B and C]. TiO₂ nanoparticles can also be formed through the thermal oxidation of MXene, thereby substantially enhancing the thermal stability of such a hybrid protective layer. For gas-phase flame retardancy, as discussed above, gases containing H₂O, CO, CO₂ and NH₃ can be induced by the thermal degradation and dehydration processes of functional groups and rapidly diffuse to the epidermis of the PCNF/CS-M films. Two positive effects can be achieved: (i) diluting the concentration of oxygen^[42]; and (ii) cooling the surface temperature^[43], which largely weaken the damage from the flame

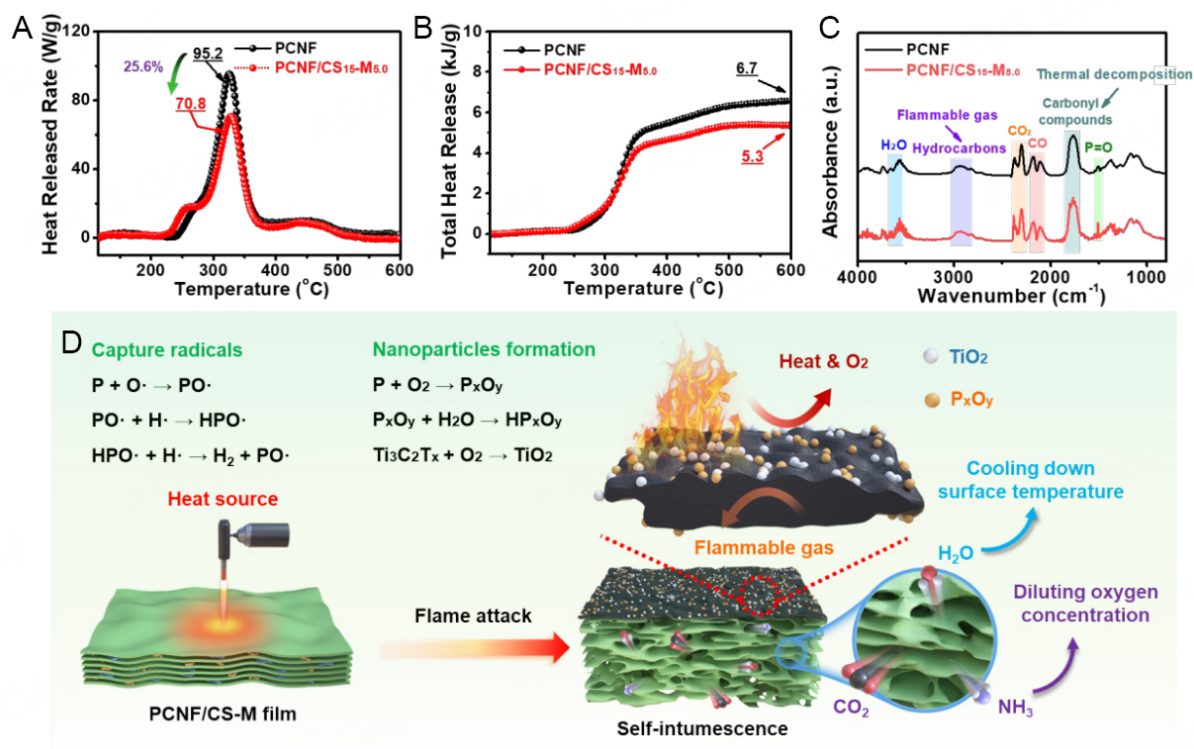


Figure 6. Analysis of flame-retardant mechanism. (A) HRR and (B) THR versus temperature curves and (C) FTIR spectra of PCNF and PCNF/CS₁₅-M_{5.0} film pyrolysis products. (D) Schematic illustration of proposed flame-retardant mechanism of PCNF/CS-M film under flame attack.

attack and prolong the lifespan of the protective layer. Consequently, an effective heat and oxygen barrier effect stemming from the hybrid protective layer can be achieved successfully, resulting in the highly improved flame retardancy of the PCNF/CS-M films.

CONCLUSIONS

Mechanically flexible and flame-retardant composite films composed of phosphorylated cellulose nanofibrils, MXene and chitosan were prepared in this work via a facile method. Owing to the synergistic effect of additional hydrogen bonds (chitosan) and nanoparticle reinforcement (MXene), the resultant films exhibit preferable mechanical properties (e.g., tensile strength of 172.1 MPa and toughness of 8.5 MJ/m³) by accommodating material components, which are superior to those of the one strengthened by a single strategy. Additionally, the PCNF/CS-M films also possess extraordinary thermal stability under cyclic flame testing at high temperature (700-800 °C), which is further proved by the evidently decreased value of PHRR and THR, implying distinctive flame-retardant performance. With the elaborative analysis of the structural evolution results, a protective layer composed of phosphorus oxide, MXene and carbon can be rapidly formed under flame attack, thereby providing an adequate heat and oxygen barrier effect. In conclusion, this work provides a novel scenario to achieve bio-based film materials with mechanical properties and flame retardancy concurrently, which will broaden their promising applications, e.g., as fire-safety materials for fireproof coatings.

DECLARATIONS

Authors' contributions

Made substantial contributions to conception and design of the study: Li SN, Peng L, Jiang B

Performed data acquisition, analysis and interpretation: Zeng ZF, He XF, Xu ZC, Luo YH, Ni QY

Provided technical, and material support: Gong LX, Li Y

Wrote the original draft and validated the manuscript: Li SN, Peng L, Jiang B

Availability of data and materials

Not applicable.

Financial support and sponsorship

This work was supported by the National Science Foundation of China (52203148 and 12002113), Research Foundation of Talented Scholars of Zhejiang A & F University (2020FR070 and 2021FR024), Zhejiang A&F University Scientific Research Training Program for Undergraduates (S202210341186) and China Postdoctoral Science Foundation (2022T150558).

Conflicts of interest

All authors declared that there are no conflicts of interest.

Ethical approval and consent to participate

Not applicable.

Consent for publication

Not applicable.

Copyright

© The Author(s) 2022.

REFERENCES

1. Bai Y, Zhao Y, Li Y, et al. UV-shielding alginate films crosslinked with Fe³⁺ containing EDTA. *Carbohydr Polym* 2020;239:115480. DOI PubMed
2. Afzal A, Khaliq Z, Ahmad S, Ahmad F, Noor A, Qadir MB. Development and characterization of biodegradable composite film. *Environ Technol Innov* 2021;23:101664. DOI
3. Kumar S, Jahan K, Verma A, Agarwal M, Chandraprakash C. Agar-based composite films as effective biodegradable sound absorbers. *ACS Sustain Chem Eng* 2022;10:8242-53. DOI
4. Li S, Li B, Gong L, et al. Enhanced mechanical properties of polyacrylamide/chitosan hydrogels by tuning the molecular structure of hyperbranched polysiloxane. *Mater Des* 2019;162:162-70. DOI
5. Ye Y, Zhang Y, Chen Y, Han X, Jiang F. Cellulose nanofibrils enhanced, strong, stretchable, freezing-tolerant ionic conductive organohydrogel for multi-functional sensors. *Adv Funct Mater* 2020;30:2003430. DOI
6. Rol F, Belgacem MN, Gandini A, Bras J. Recent advances in surface-modified cellulose nanofibrils. *Prog Polym Sci* 2019;88:241-64. DOI
7. Li T, Li SX, Kong W, et al. A nanofluidic ion regulation membrane with aligned cellulose nanofibers. *Sci Adv* 2019;5:eaa4238. DOI PubMed PMC
8. Wang C, Wang S, Chen G, et al. Flexible, bio-compatible nanofluidic Ion conductor. *Chem Mater* 2018;30:7707-13. DOI
9. Hu J, Wu Y, Yang Q, et al. One-pot freezing-thawing preparation of cellulose nanofibrils reinforced polyvinyl alcohol based ionic hydrogel strain sensor for human motion monitoring. *Carbohydr Polym* 2022;275:118697. DOI PubMed
10. Xu D, Wang S, Berglund LA, Zhou Q. Surface charges control the structure and properties of layered nanocomposite of cellulose nanofibrils and clay platelets. *ACS Appl Mater Interfaces* 2021;13:4463-72. DOI PubMed PMC
11. Li Y, Grishkewich N, Liu L, et al. Construction of functional cellulose aerogels via atmospheric drying chemically cross-linked and solvent exchanged cellulose nanofibrils. *Chem Eng J* 2019;366:531-8. DOI
12. Ghanadpour M, Carosio F, Wågberg L. Ultrastrong and flame-resistant freestanding films from nanocelluloses, self-assembled using a layer-by-layer approach. *Appl Mater Today* 2017;9:229-39. DOI
13. Tong C, Zhang S, Zhong T, Fang Z, Liu H. Highly fibrillated and intrinsically flame-retardant nanofibrillated cellulose for transparent

- mineral filler-free fire-protective coatings. *Chem Eng J* 2021;419:129440. DOI
14. Farooq M, Sipponen MH, Seppälä A, Österberg M. Eco-friendly flame-retardant cellulose nanofibril aerogels by incorporating sodium bicarbonate. *ACS Appl Mater Interfaces* 2018;10:27407-15. DOI PubMed PMC
 15. Ghanadpour M, Carosio F, Ruda MC, Wågberg L. Tuning the nanoscale properties of phosphorylated cellulose nanofibril-based thin films to achieve highly fire-protecting coatings for flammable solid materials. *ACS Appl Mater Interfaces* 2018;10:32543-55. DOI PubMed
 16. Li S, Yu Z, Guo B, et al. Environmentally stable, mechanically flexible, self-adhesive, and electrically conductive Ti3C2TX MXene hydrogels for wide-temperature strain sensing. *Nano Energy* 2021;90:106502. DOI
 17. Mao M, Yu K, Cao C, et al. Facile and green fabrication of flame-retardant Ti3C2Tx MXene networks for ultrafast, reusable and weather-resistant fire warning. *Chem Eng J* 2022;427:131615. DOI
 18. Shimizu M, Fukuzumi H, Saito T, Isogai A. Preparation and characterization of TEMPO-oxidized cellulose nanofibril films with free carboxyl groups. *Carbohydr Polym* 2011;84:579-583. DOI
 19. Li Y, Chen Y, He X, Xiang Z, Heinze T, Qi H. Lignocellulose nanofibril/gelatin/MXene composite aerogel with fire-warning properties for enhanced electromagnetic interference shielding performance. *Chem Eng J* 2022;431:133907. DOI
 20. Zhang S, Li S, Wu Q, et al. Phosphorus containing group and lignin toward intrinsically flame retardant cellulose nanofibril-based film with enhanced mechanical properties. *Compos Part B Eng* 2021;212:108699. DOI
 21. Dong L, Hu C, Song L, Huang X, Chen N, Qu L. A large-area, flexible, and flame-retardant graphene paper. *Adv Funct Mater* 2016;26:1470-6. DOI
 22. Hou G, Zhao S, Li Y, Fang Z, Isogai A. Mechanically robust, flame-retardant phosphorylated cellulose films with tunable optical properties for light management in LEDs. *Carbohydr Polym* 2022;298:120129. DOI PubMed
 23. Tao Y, Huang C, Lai C, Huang C, Yong Q. Biomimetic galactomannan/bentonite/graphene oxide film with superior mechanical and fire retardant properties by borate cross-linking. *Carbohydr Polym* 2020;245:116508. DOI PubMed
 24. Yu ZR, Li SN, Zang J, et al. Enhanced mechanical property and flame resistance of graphene oxide nanocomposite paper modified with functionalized silica nanoparticles. *Compos Part B Eng* 2019;177:107347. DOI
 25. Cao C, Yu B, Guo B, et al. Bio-inspired, sustainable and mechanically robust graphene oxide-based hybrid networks for efficient fire protection and warning. *Chem Eng J* 2022;439:134516. DOI
 26. Cao CF, Yu B, Chen ZY et al. Fire intumescent, high-temperature resistant, mechanically flexible graphene oxide network for exceptional fire shielding and ultra-fast fire warning. *Nano-Micro Lett* 2022;14:92. DOI PubMed PMC
 27. Phanthuwongpakdee J, Harimoto T, Babel S, Dwivedi S, Takada K, Kaneko T. Flame retardant transparent films of thermostable biopolyimide metal hybrids. *Polym Degrad Stab* 2021;188:109571. DOI
 28. Lopez V, Paton-carrero A, Romero A, Valverde JL, Sanchez-silva L. Improvement of the mechanical and flame-retardant properties of polyetherimide membranes modified with Graphene oxide. *Polym-Plast Tech Mat* 2019;58:1170-7. DOI
 29. Li J, Wang S, Liu F, et al. Flame-retardant AEMs based on organic-inorganic composite polybenzimidazole membranes with enhanced hydroxide conductivity. *J Membr Sci* 2019;591:117306. DOI
 30. Yu Z, Mao M, Li S, et al. Facile and green synthesis of mechanically flexible and flame-retardant clay/graphene oxide nanoribbon interconnected networks for fire safety and prevention. *Chem Eng J* 2021;405:126620. DOI
 31. Chen G, Hu Y, Peng F, et al. Fabrication of strong nanocomposite films with renewable forestry waste/montmorillonite/reduction of graphene oxide for fire retardant. *Chem Eng J* 2018;337:436-45. DOI
 32. Li K, Skolrood LN, Aytug T, Tekinalp H, Ozcan S. Strong and tough cellulose nanofibrils composite films: mechanism of synergetic effect of hydrogen bonds and ionic interactions. *ACS Sustain Chem Eng* 2019;7:14341-6. DOI
 33. Cao W, Ma C, Mao D, Zhang J, Ma M, Chen F. MXene-reinforced cellulose nanofibril inks for 3D-printed smart fibres and textiles. *Adv Funct Mater* 2019;29:1905898. DOI
 34. Huo S, Zhou Z, Jiang J, et al. Flame-retardant, transparent, mechanically-strong and tough epoxy resin enabled by high-efficiency multifunctional boron-based polyphosphonamide. *Chem Eng J* 2022;427:131578. DOI
 35. Li S, He X, Zeng Z, et al. Mechanically ductile, ionically conductive and low-temperature tolerant hydrogel enabled by high-concentration saline towards flexible strain sensor. *Nano Energy* 2022;103:107789. DOI
 36. Wang T, Long M, Zhao H, et al. Temperature-responsive intumescent chemistry toward fire resistance and super thermal insulation under extremely harsh conditions. *Chem Mater* 2021;33:6018-28. DOI
 37. Miao J, Yuan L, Guan Q, Liang G, Gu A. Biobased heat resistant epoxy resin with extremely high biomass content from 2,5-furandicarboxylic acid and eugenol. *ACS Sustain Chem Eng* 2017;5:7003-11. DOI
 38. Shi Q, Huo S, Wang C, et al. A phosphorus/silicon-based, hyperbranched polymer for high-performance, fire-safe, transparent epoxy resins. *Polym Degrad Stab* 2022;203:110065. DOI
 39. Sai T, Su Y, Shen H, et al. Fabrication and mechanism study of cerium-based P, N-containing complexes for reducing fire hazards of polycarbonate with superior thermostability and toughness. *ACS Appl Mater Interfaces* 2021;30061-75. DOI PubMed
 40. Xue Y, Feng J, Huo S, et al. Polyphosphoramidate-intercalated MXene for simultaneously enhancing thermal stability, flame retardancy and mechanical properties of polylactide. *Chem Eng J* 2020;397:125336. DOI
 41. Velencoso MM, Battig A, Markwart JC, Schartel B, Wurm FR. Molecular firefighting-how modern phosphorus chemistry can help solve the challenge of flame retardancy. *Angew Chem Int Ed Engl* 2018;57:10450-67. DOI PubMed PMC
 42. Teng N, Dai J, Wang S, Hu J, Liu X. Hyperbranched flame retardant for epoxy resin modification: simultaneously improved flame

- retardancy, toughness and strength as well as glass transition temperature. *Chem Eng J* 2022;428:131226. [DOI](#)
43. Chen L, Zhao D, Wang X, Wang Y. Durable macromolecular firefighting for unsaturated polyester via integrating synergistic charring and hydrogen bond. *Chem Eng J* 2022;443:136365. [DOI](#)